

CORSO DI:

ELABORAZIONE DI SEGNALI BIOMEDICI

(LUCIDI DELLE LEZIONI III)

PROF. SERGIO CERUTTI

Dipartimento di Bioingegneria

Politecnico di Milano

OTTOBRE 2004

VARIABILITÀ CARDIACA

Cenni storici

Hales (1733)

Ludwig (1847)

Traube (1865)

Hering (1869)

Cion (1874)

Mayer (1876)

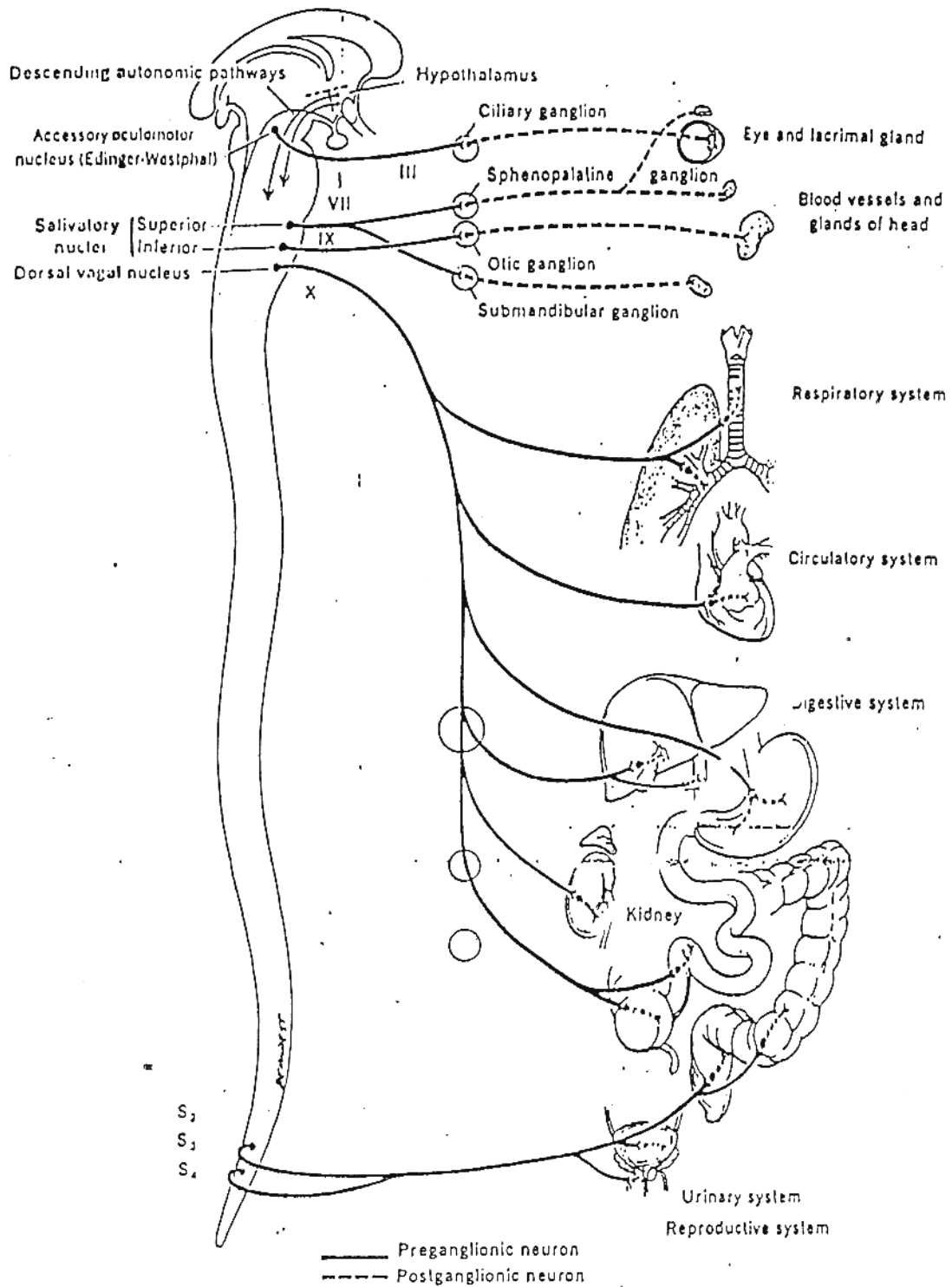
Marey / Lippmann (1876)

Elettrometro capillare

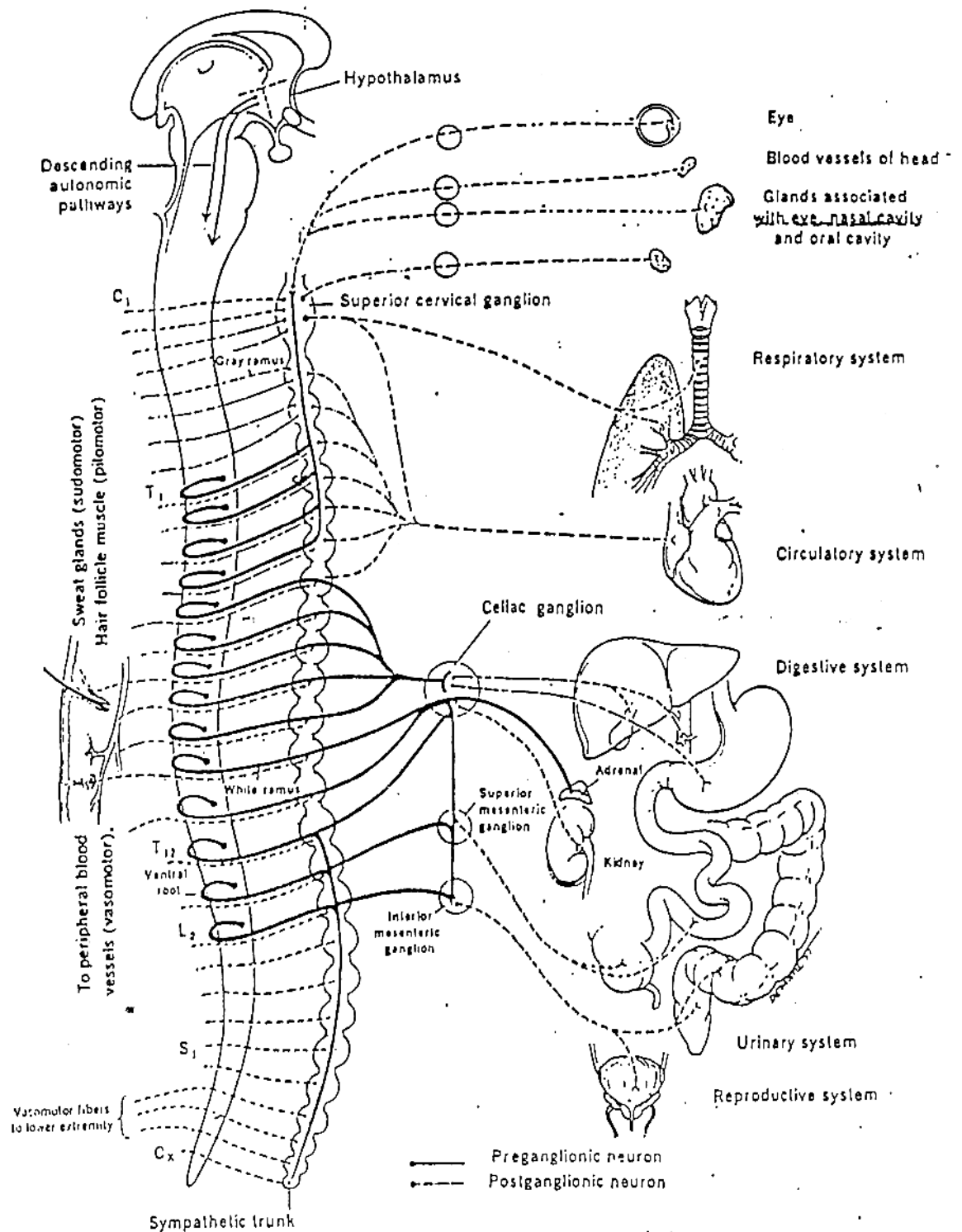
Einthoven (1903)

Galvanometro a corda

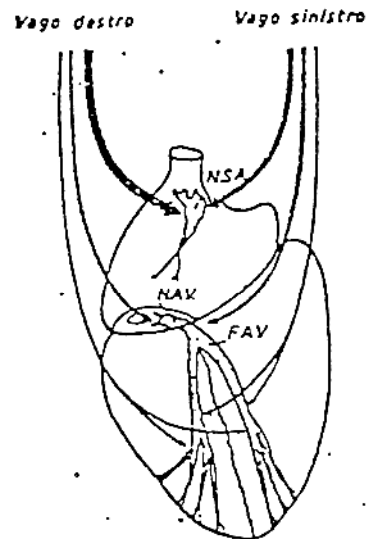
SISTEMA PARASIMPATICO



SISTEMA ORTOSIMPATICO (SIMPATICO)



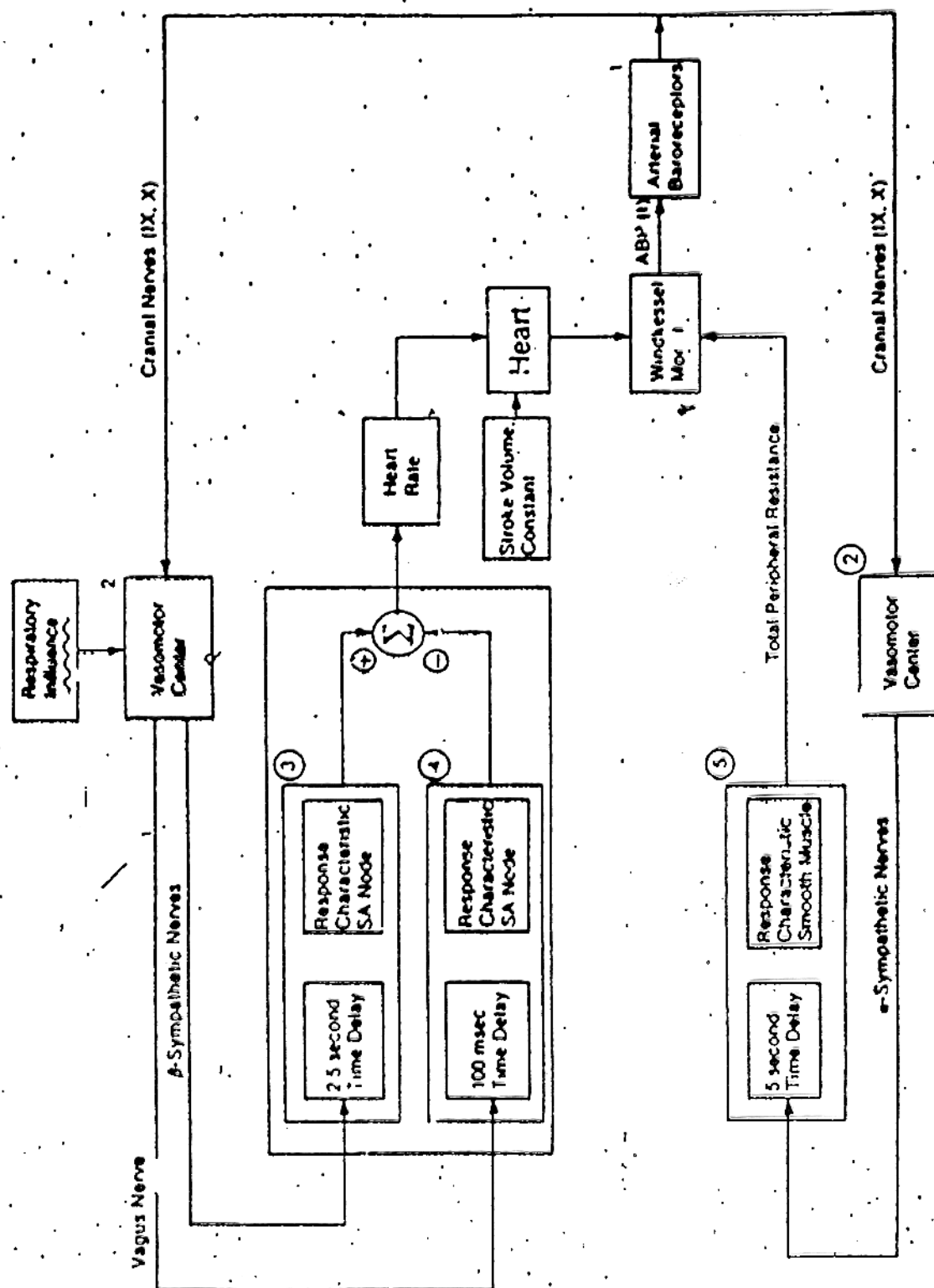
ATTIVITÀ DEL VAGO

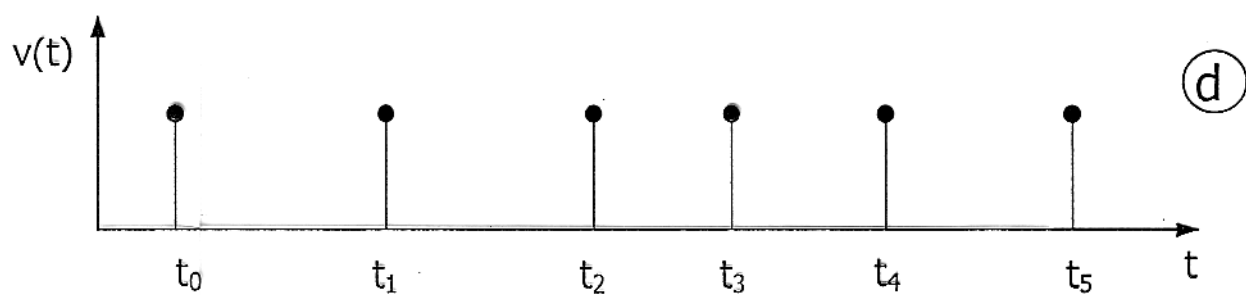
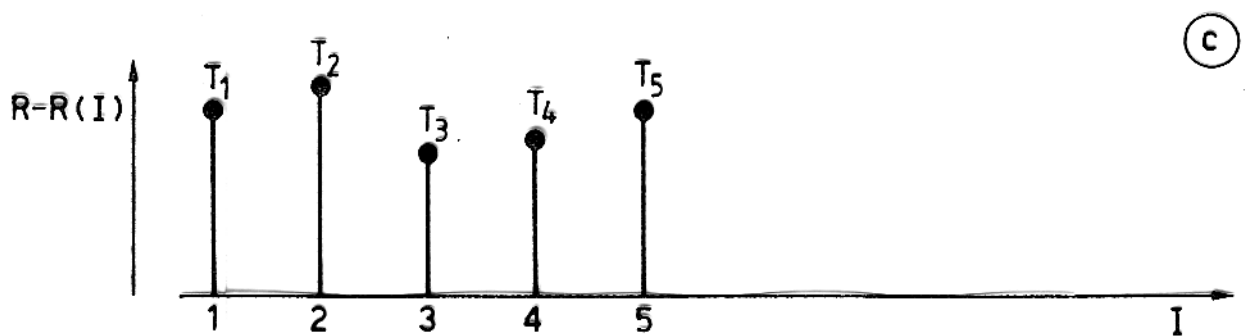
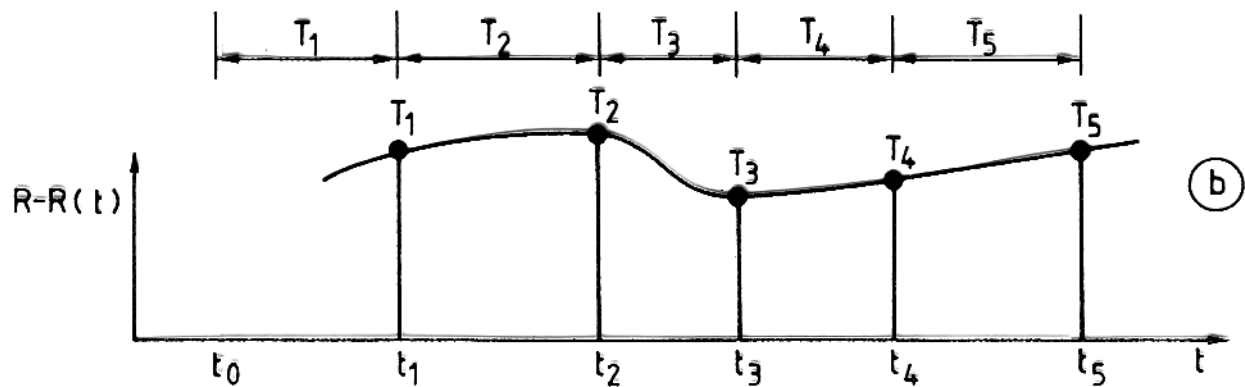
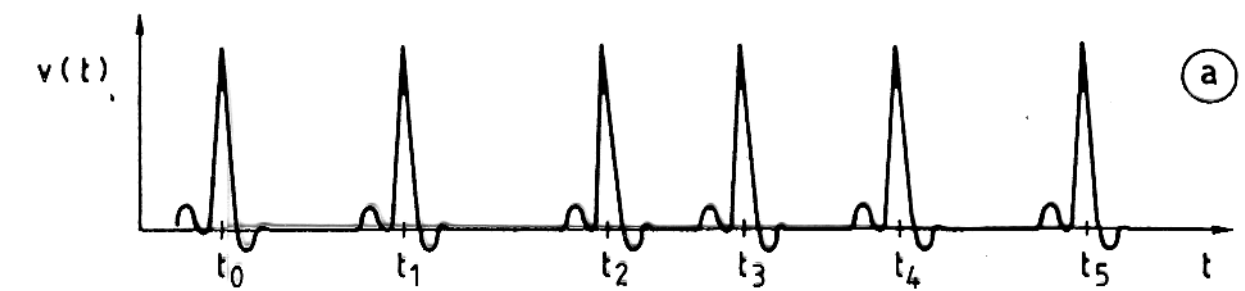


- ▼ FREQUENZA
- ▼ CONTRATTILITA'
- ▼ CONDUCIBILITA'
- ▼ ECCITABILITA'

Distribuzione delle terminazioni del vago destro e sinistro lungo il sistema di eccitamento e di conduzione del cuore.

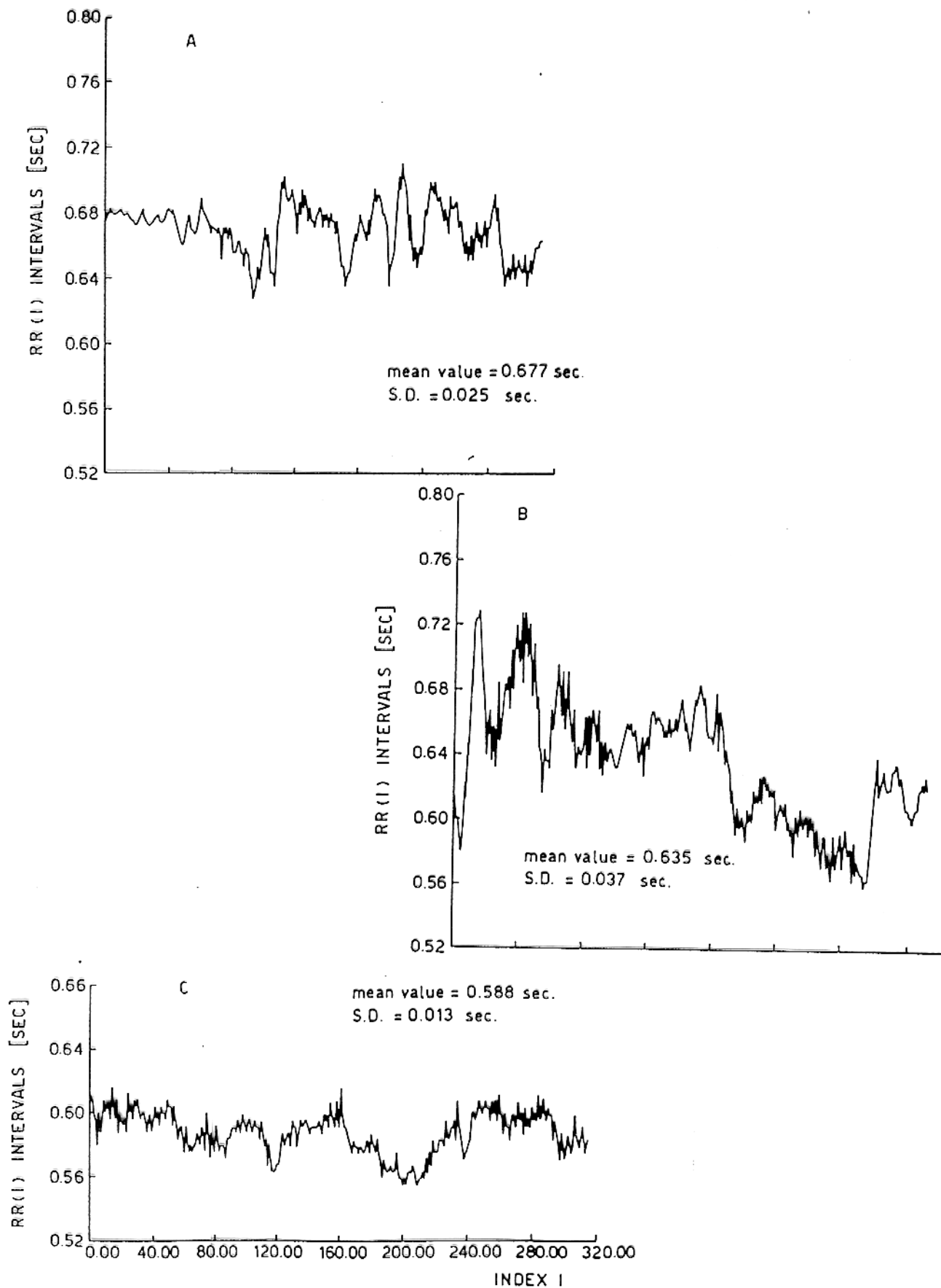
N.S.A., Nodo seno-atriale di Keith e FLACK; *N.A.V.*, nodo atrio-ventricolare di TAWARA; *F.A.V.*, fascio atrio-ventricolare di HIS.





(a) Segnale ECG originale, (b) funzione degli intervalli , (c) tacogramma, (d) funzioni delta di Dirac (point processes)

TACOGRAMMI DEGLI INTERVALLI R-R



ISTOGRAMMI

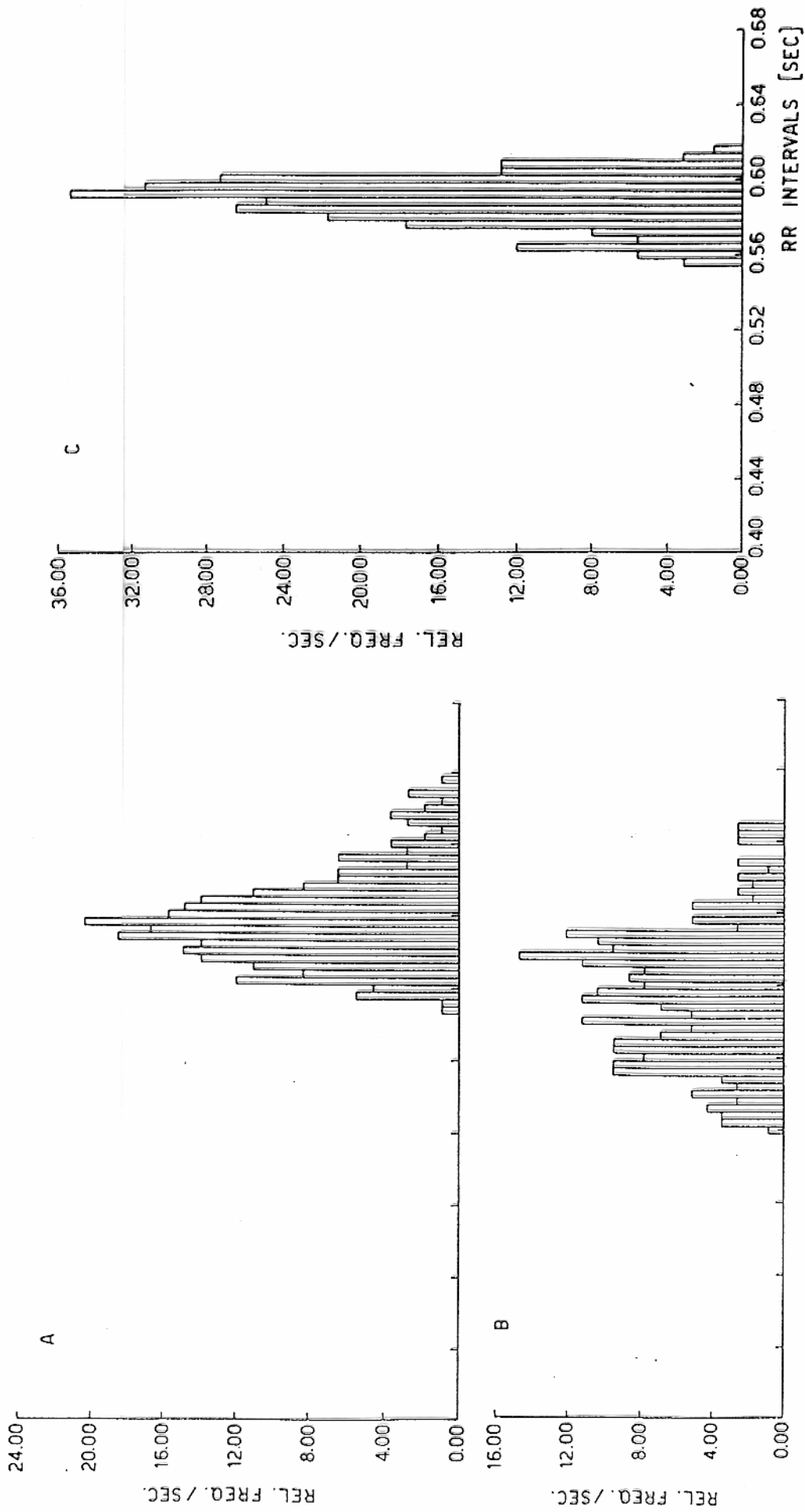


Fig. 4. Histogram of the R-R intervals referred to a patient in periods A, B, C (see text).

SCATTERGRAMMI

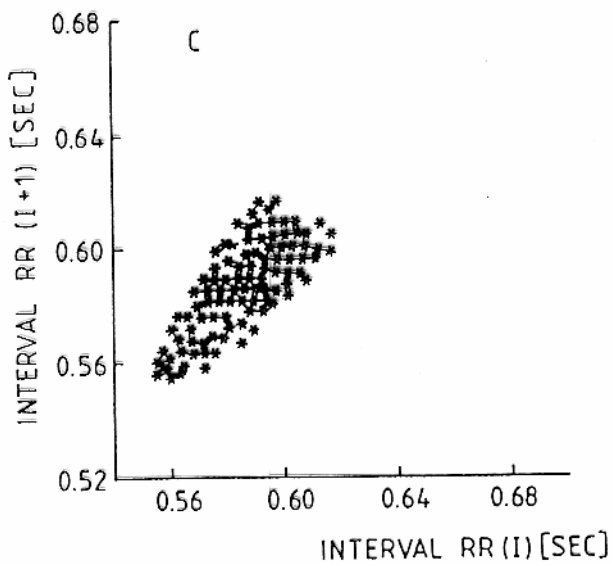
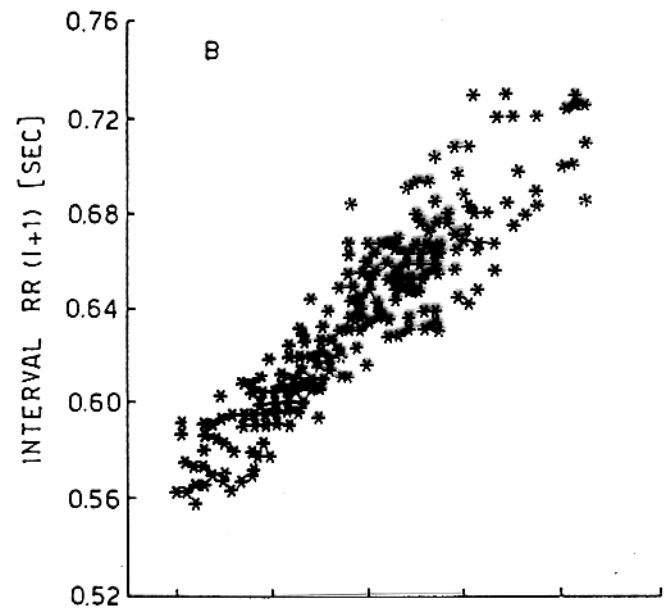
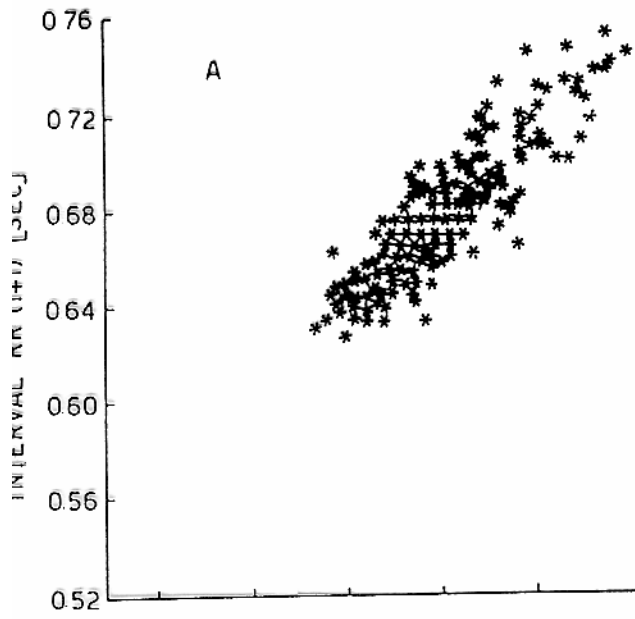
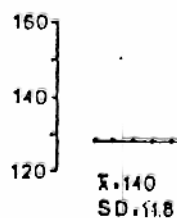
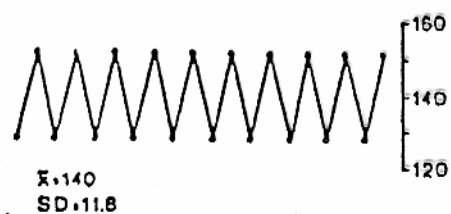
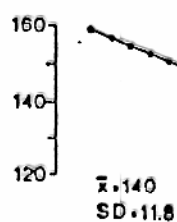


Fig. 5. Display of $(R-R)_i$ vs. $(R-R)_{i+1}$ intervals (scattergrams) for the predetermined time length.

SERIE TEMPORALI CON UGUALE VARIANZA



STIMA DELLO SPETTRO

(metodo non parametrico)

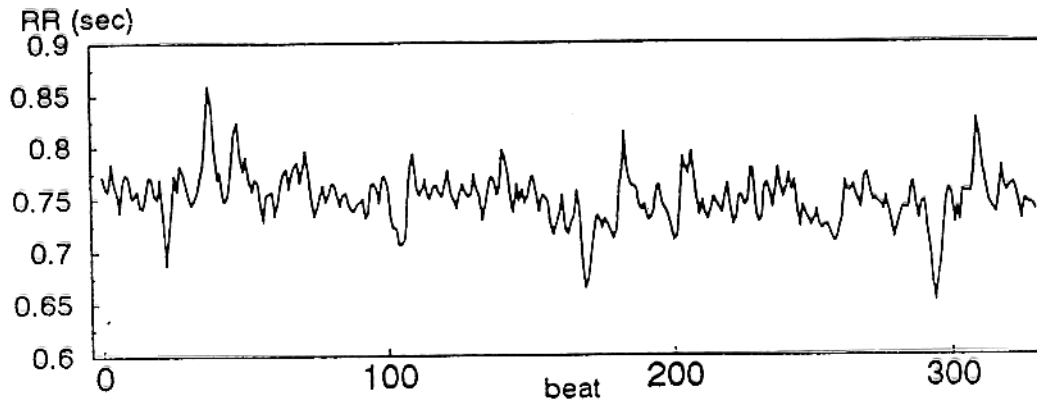
$$P_Y(f) = \frac{1}{N\Delta t} \left| \Delta t \sum_{k=0}^{N-1} y(k) \cdot \exp(-j2\pi f k \Delta t) \right|^2 = \frac{1}{N\Delta t} |Y(f_m)|^2$$

$$f_m = m \cdot \Delta f \quad \Delta f = \frac{1}{N\Delta T} \quad m = 0, 1, \dots, N-1$$

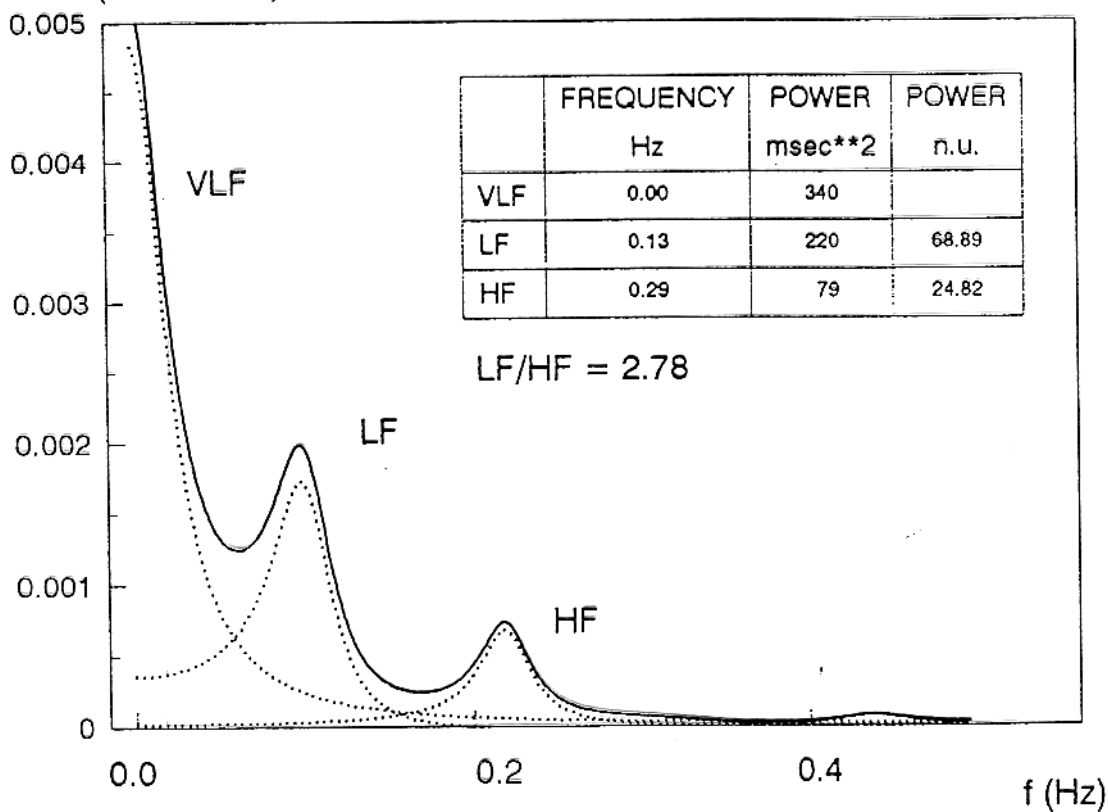
$$P_{XY}(f) = \frac{1}{N\Delta t} X(f) \cdot Y(f_m)^* = G_{XY}(f) \cdot \exp(j\Phi_{XY}(f))$$

$$k_{XY}^2(f) = \frac{G_{XY}(f)^2}{P_X(f) \cdot P_Y(f)}$$

ANALISI SPETTRALE: METODO PARAMETRICO

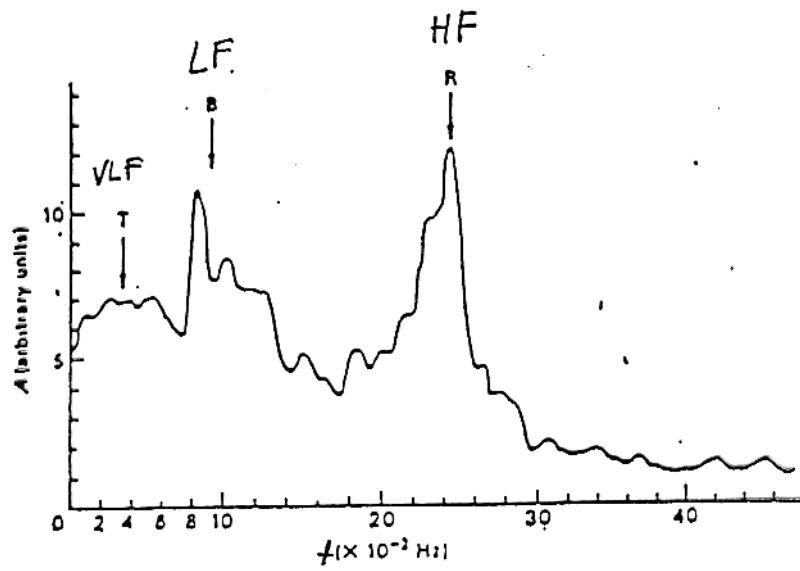


PSD (sec**2/Hz)



ANALISI SPETTRALE CLASSICA

(Sayers et al. 1973)



REST E TILT NORMALE

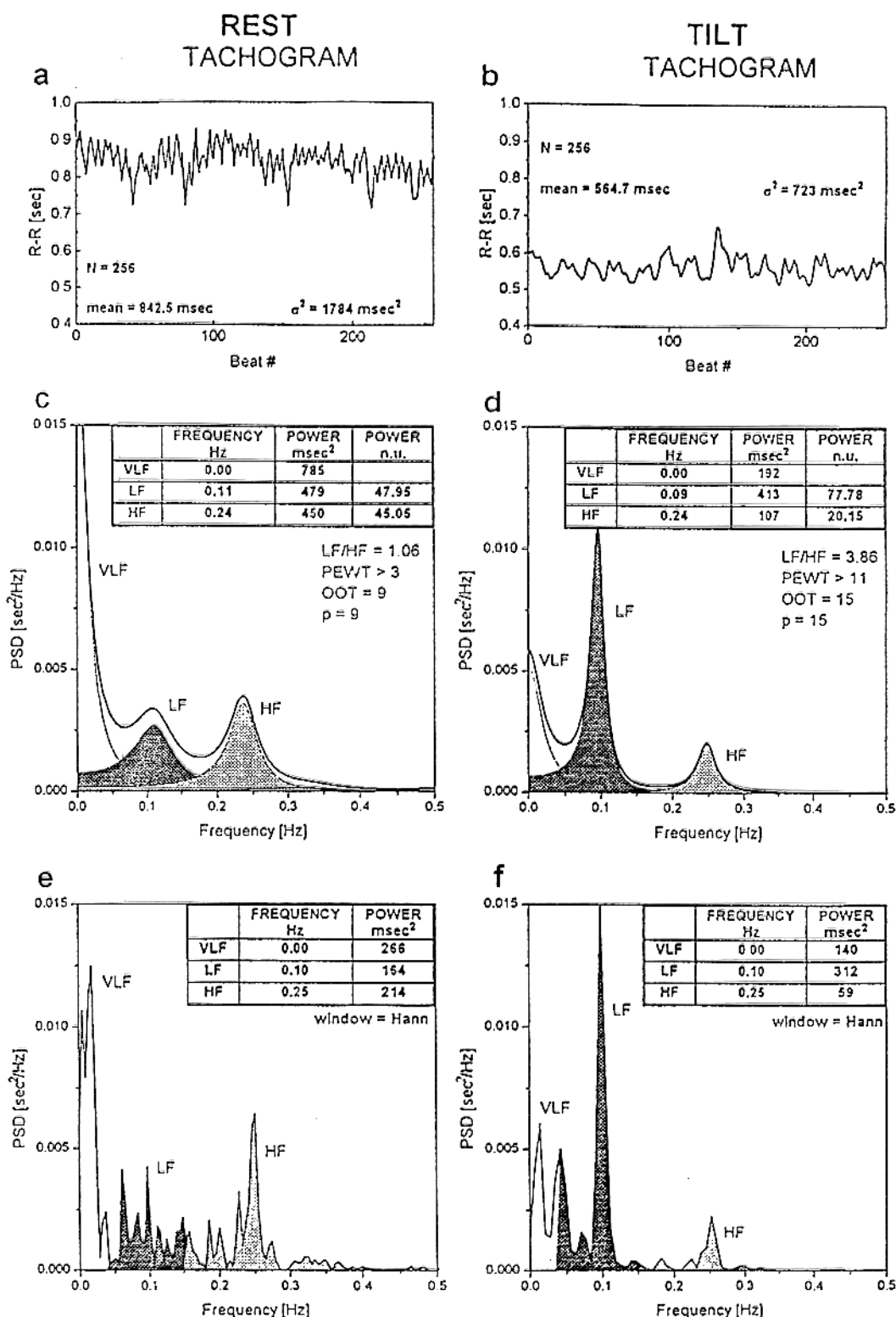


FIG 5. Interval tachogram of 256 consecutive RR values in a normal subject at supine rest (a) and after head-up tilt (b). The HRV spectra are shown, calculated by parametric autoregressive modeling (c and d) and by a fast Fourier transform-based nonparametric algorithm (e and f). Mean values (m), variances (s^2), and the number (N) of samples are indicated. For c and d, VLF, LF, and HF central frequency, power in absolute value and power in normalized units (n.u.) are also indicated together with the order p of the chosen model and minimal values of the prediction error whiteness test (PEWT) and optimal order test (OOT) that satisfy the tests. In e and f, the peak frequency and the power of VLF, LF, and HF were calculated by integrating the power spectral density (PSD) in the defined frequency bands. The window type is also specified. In c through f, the LF component is indicated by dark shaded areas and the HF component by light shaded areas.

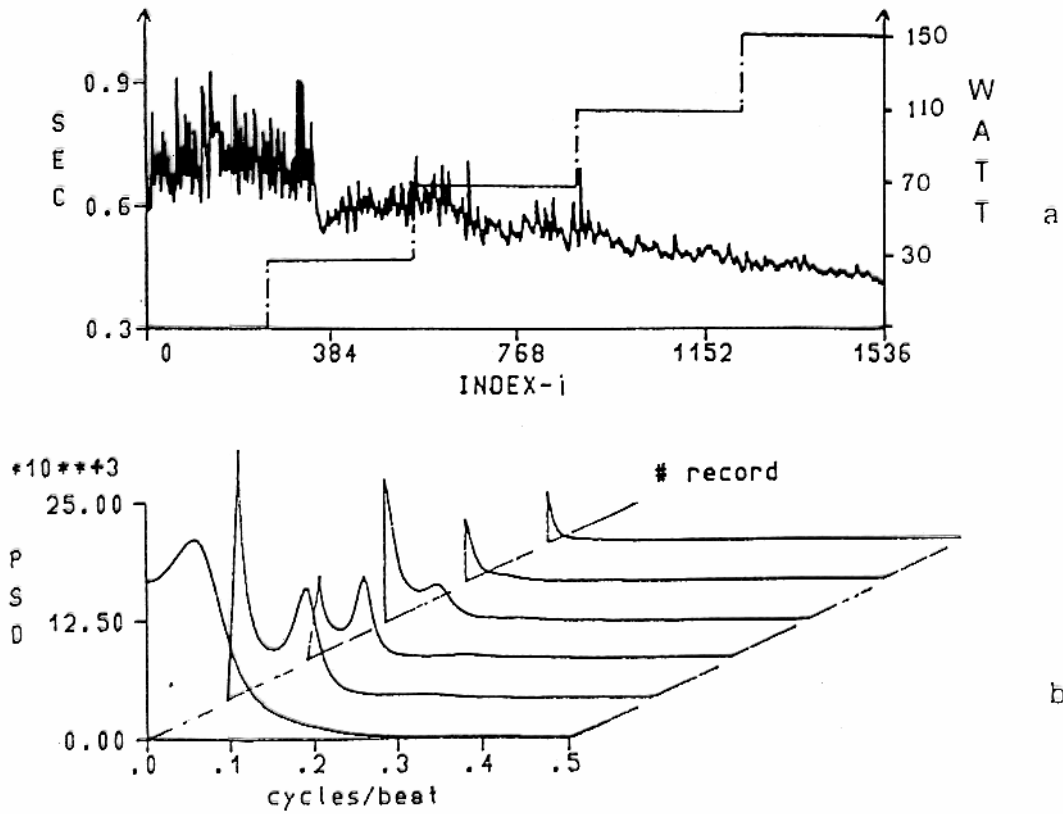


Fig. 9. Tachogram (1536 beats) of a normal subject under stress test (cycloergometer) in five different load conditions (expressed in W on the right axis) (a). Tachogram spectra calculated via AR identification on consecutive records of 256 samples for a total number of 6 spectra (b) shown in a pseudo-tridimensional way.

REST E TILT PATOLOGICO

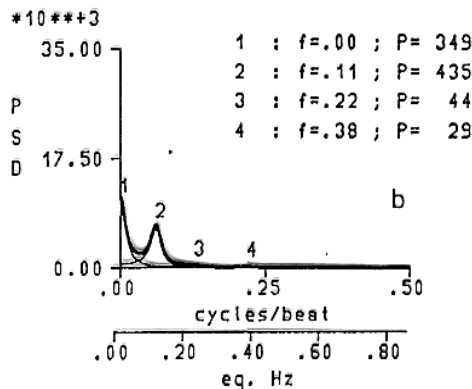
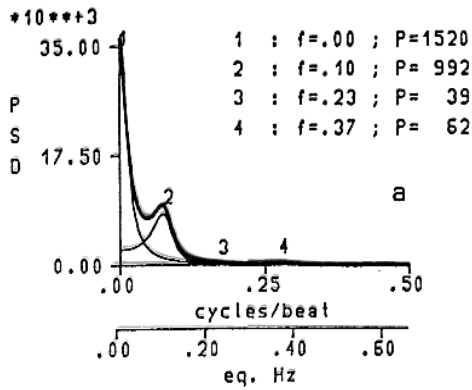


Fig. 6. As in Fig. 5 for a hypertensive subject in resting (a) and tilt (b) conditions.

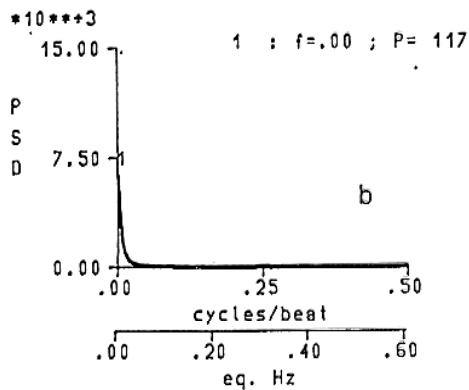
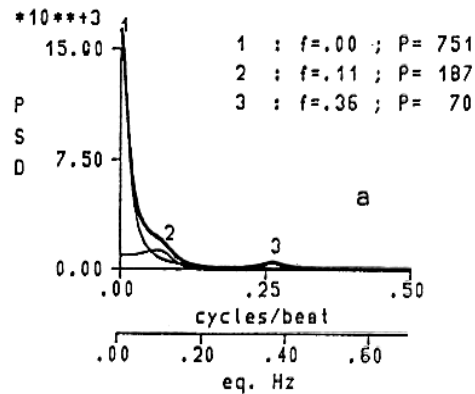


Fig. 7. Diabetic patients in resting conditions: uncomplicated case (a) and case with neuropathy (b).

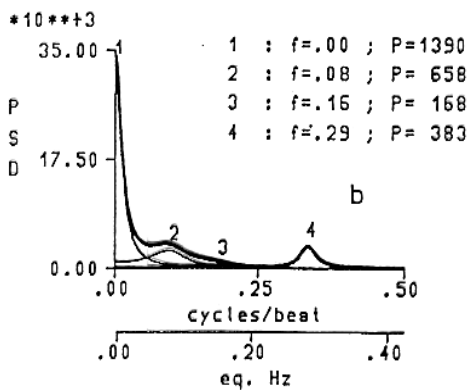
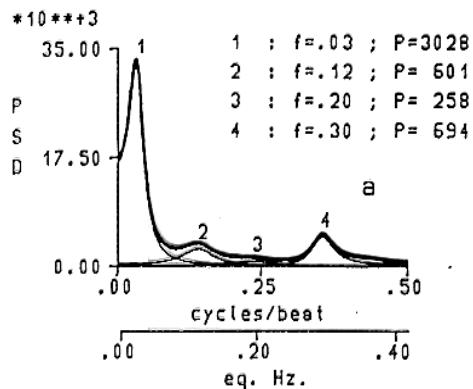


Fig. 8. PSD of a patient 15 days (a) and 6 months (b) after acute myocardial infarction.

ECG Fetale

Enhancement of Fetal ECG on Abdominal Lead by Means of Digital Filtering and Averaging Techniques

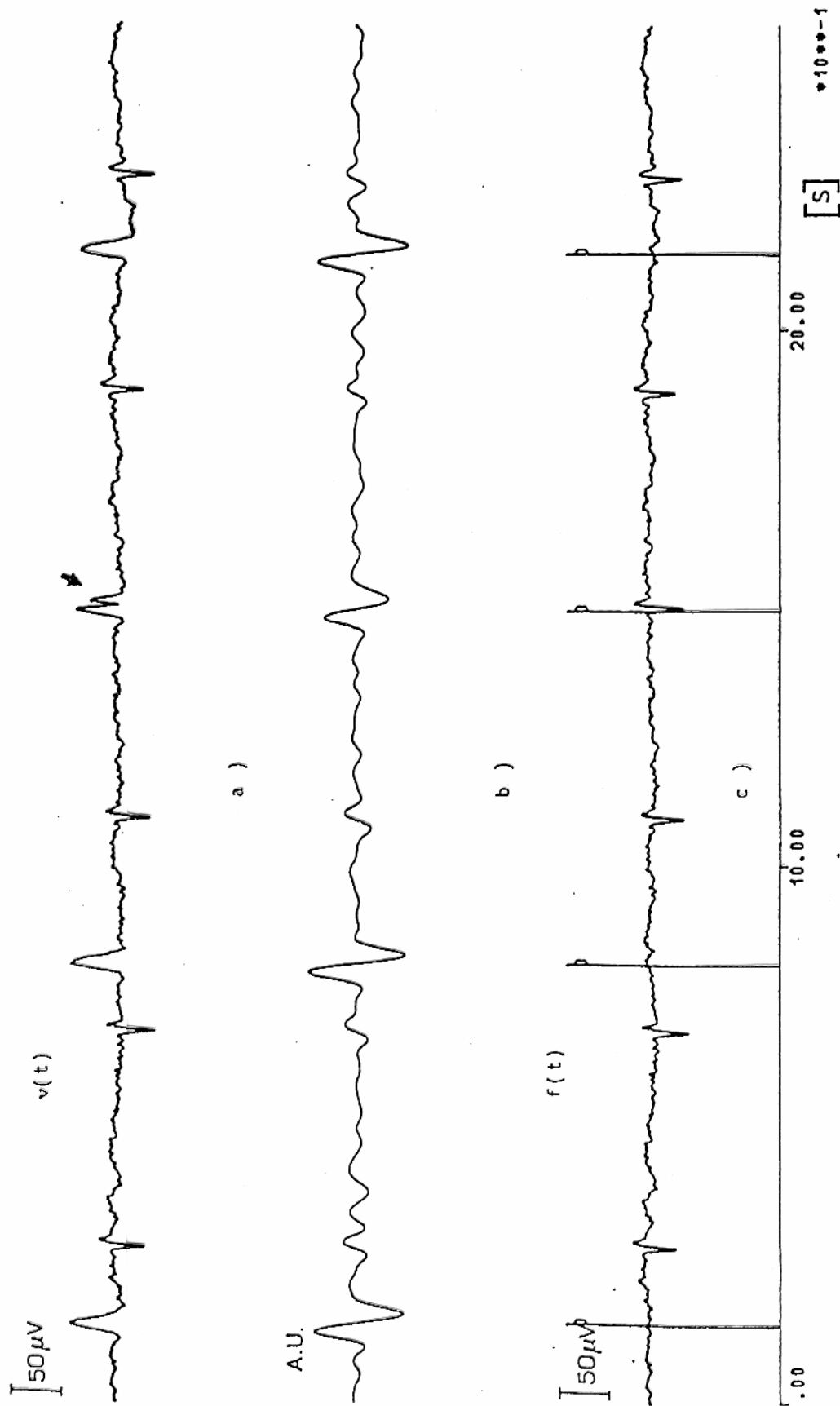


Fig. 3 - Abdominal ECG lead $v(t)$ with a case of superimposition of maternal and fetal complexes indicated with an arrow (a), filtered signal in arbitrary units (A.U.) for MQRS recognitions (b), signal $f(t)$ obtained after the subtraction of the maternal template (c).

ECG Fetale

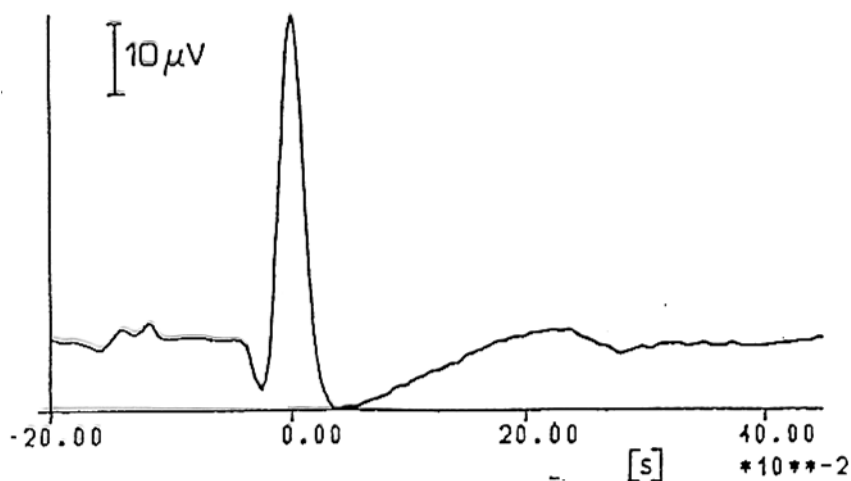


Fig. 2 - Maternal template obtained from a successive averaging on $v(t)$ signal synchronized with the maxima of MQRS and with a temporal window of 200 ms before and 450 ms after the instants of occurrence of MQRS's.

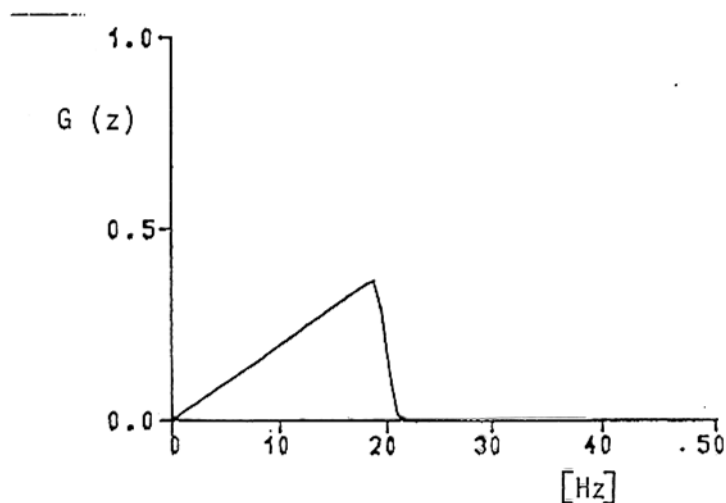


Fig. 1 - Characteristics of derivative and low-pass FIR digital filter (128 coefficients, Weber-Cappellini window, 20 Hz cutoff frequency) used for MQRS recognitions.

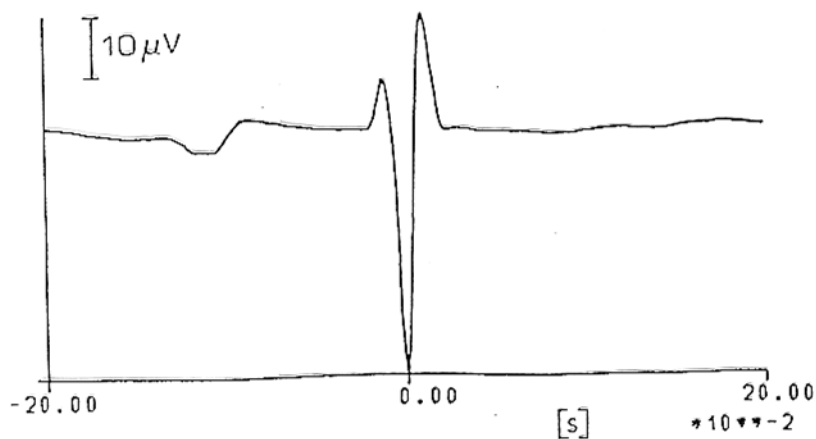


Fig. 4 - Fetal cardiac cycle obtained after a further averaging of signal $f(t)$ shown in Fig. 3c with a symmetrical temporal window of 400 ms centered on the instants of occurrence of FQRS's. Fetal P wave and QRS complex are clearly visible.

Variabilità cardiaca fetale

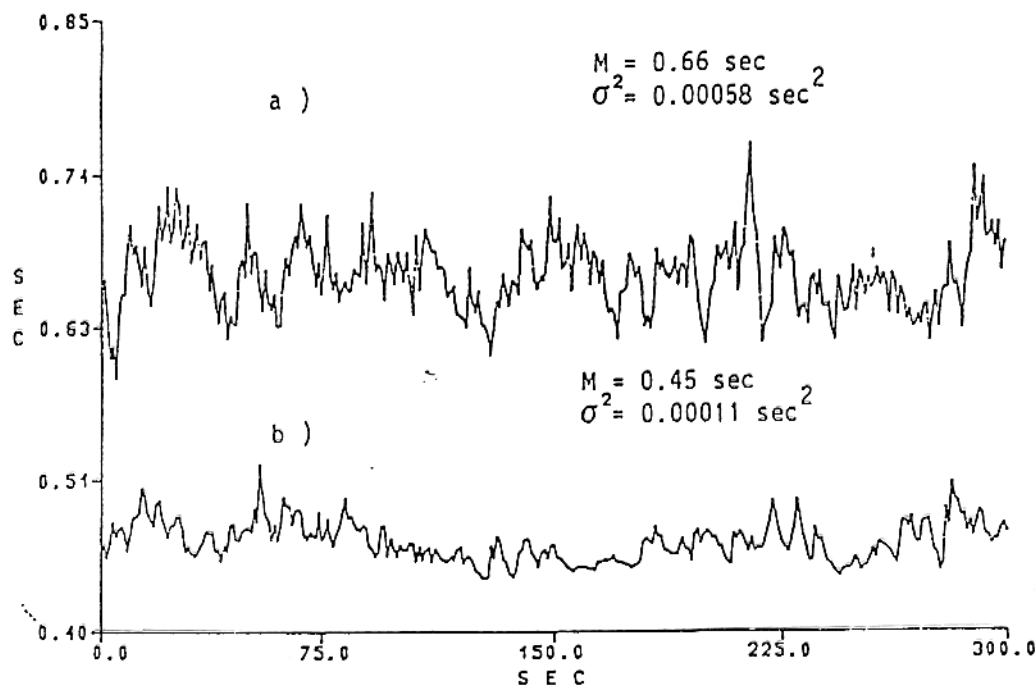


Figure 4. Maternal (a) and fetal (b) LPFES's for a total period of 5 minutes. The horizontal axis indicates the time (s) while the vertical one shows the instantaneous R-R duration after the low pass filtering illustrated in figure 3 c.

The mean value M and the variance σ^2 of the two signals are typed in the figure.

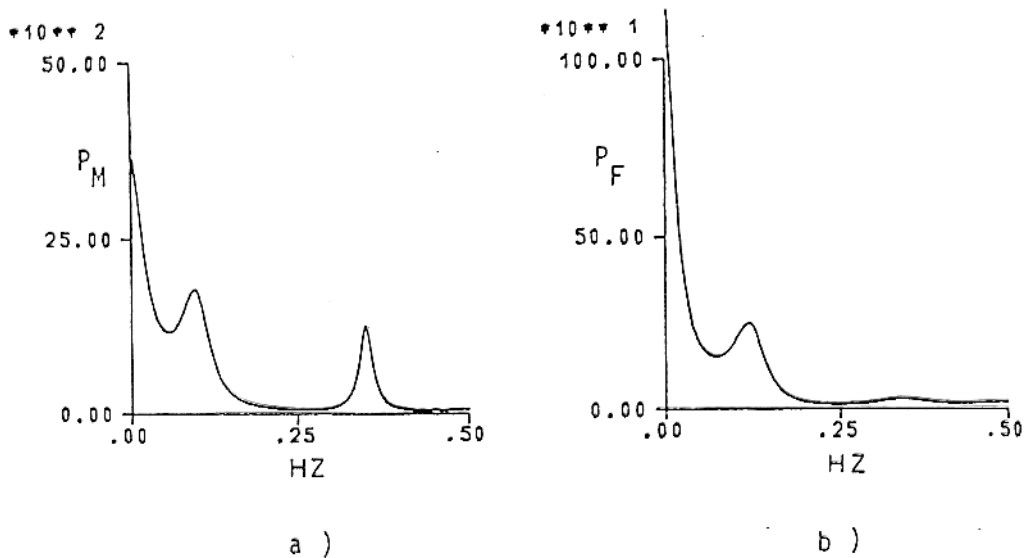
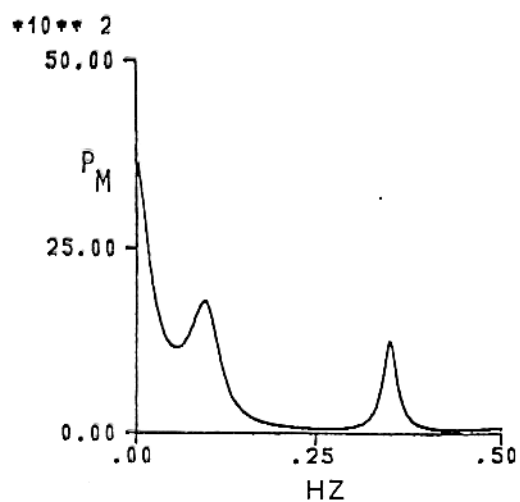
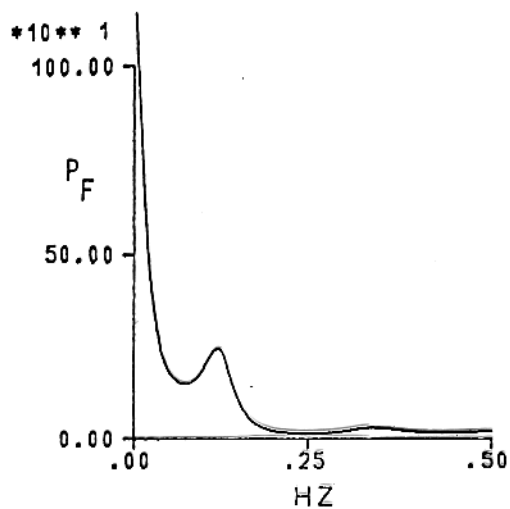


Figure 5. Power spectral density of maternal (a) and fetal (b) LPFES's.

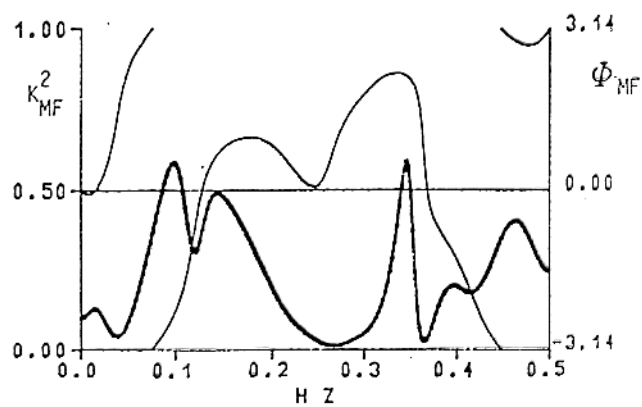
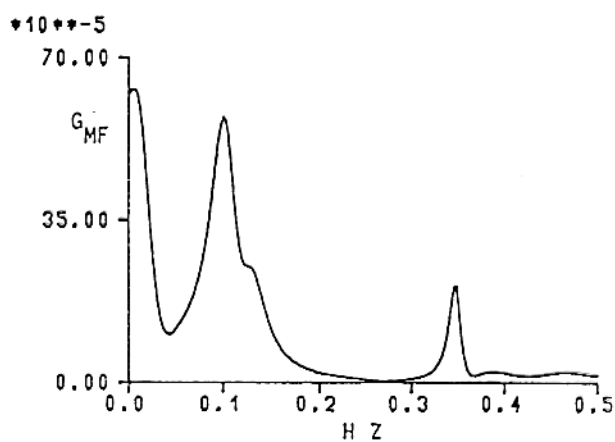
Variabilità cardiaca fetale



a)

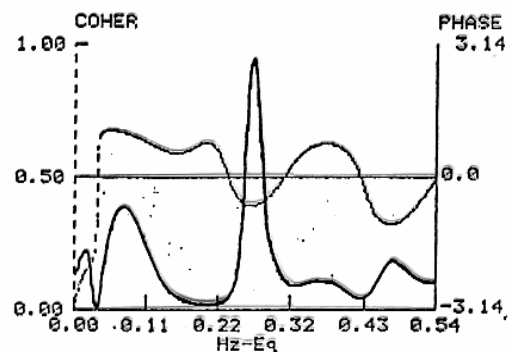
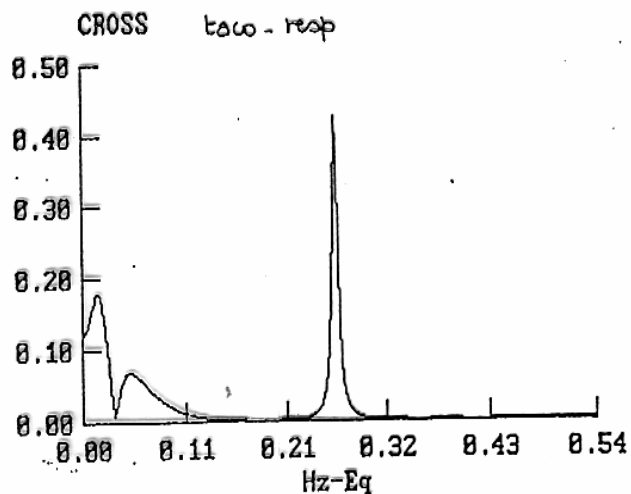


b)

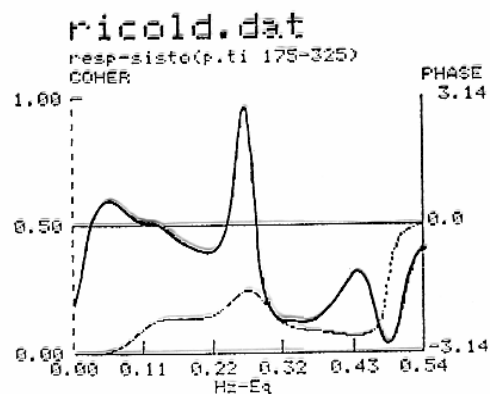
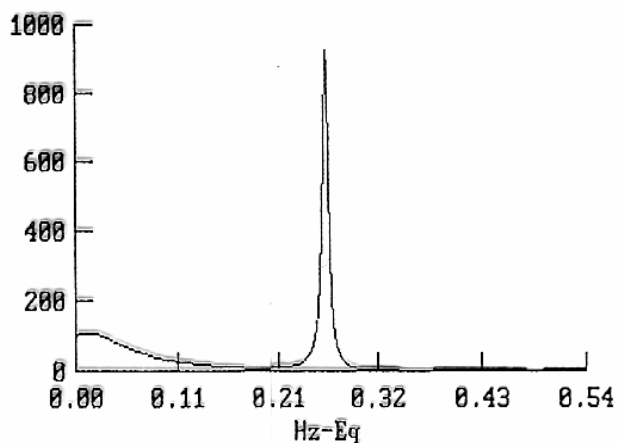


Variabilità cardiaca fetale

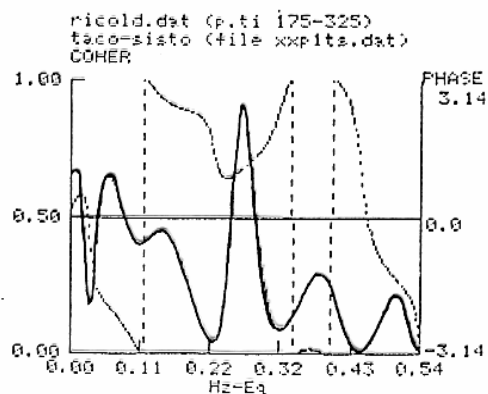
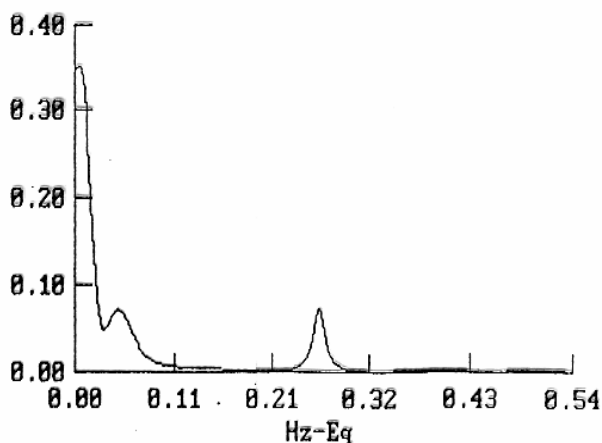
respiro



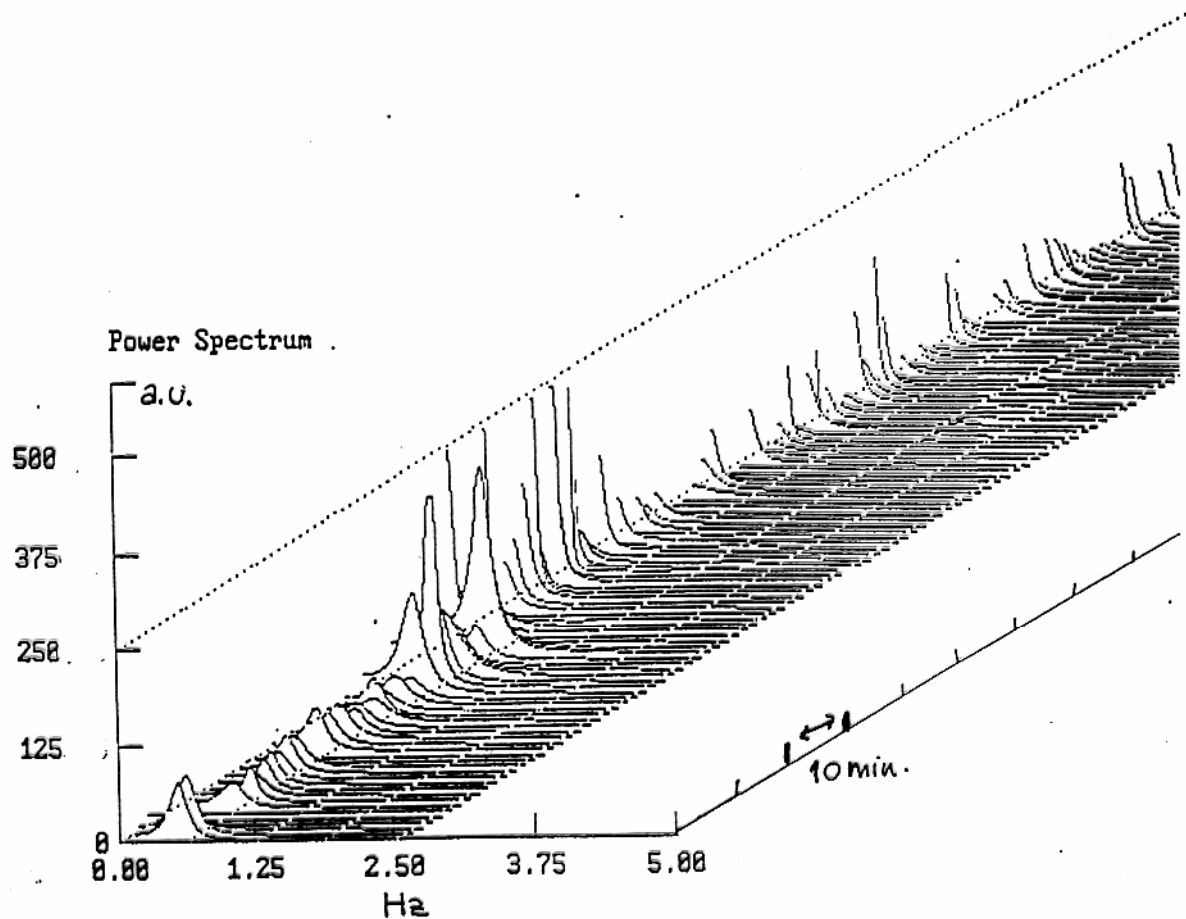
ricold.dat (p.ti 175-325)
resp-sisto (file xxp1rs.dat)
CROSS



ricold.dat (pti 175-325)
taco-sisto (file xxp1ts.dat)
CROSS



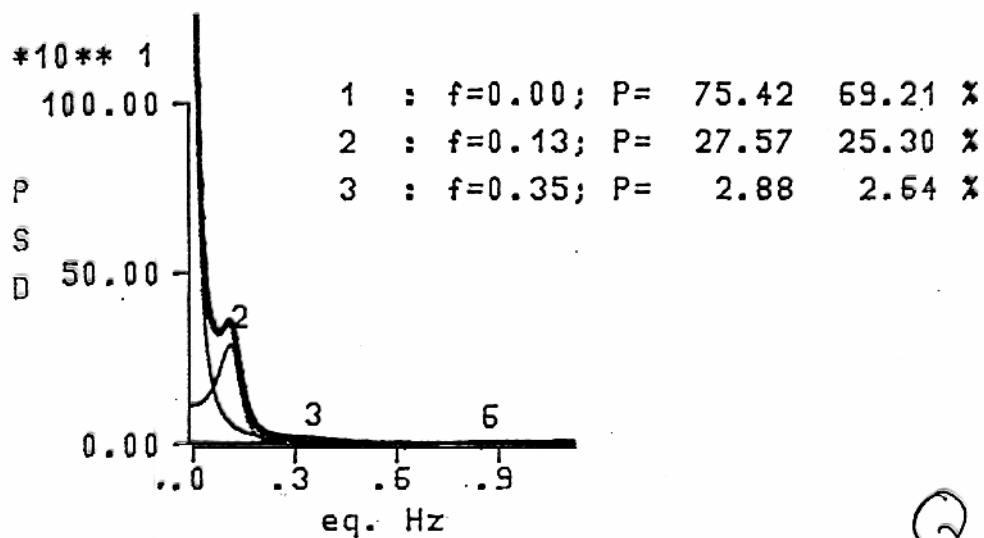
Variabilità cardiaca fetale



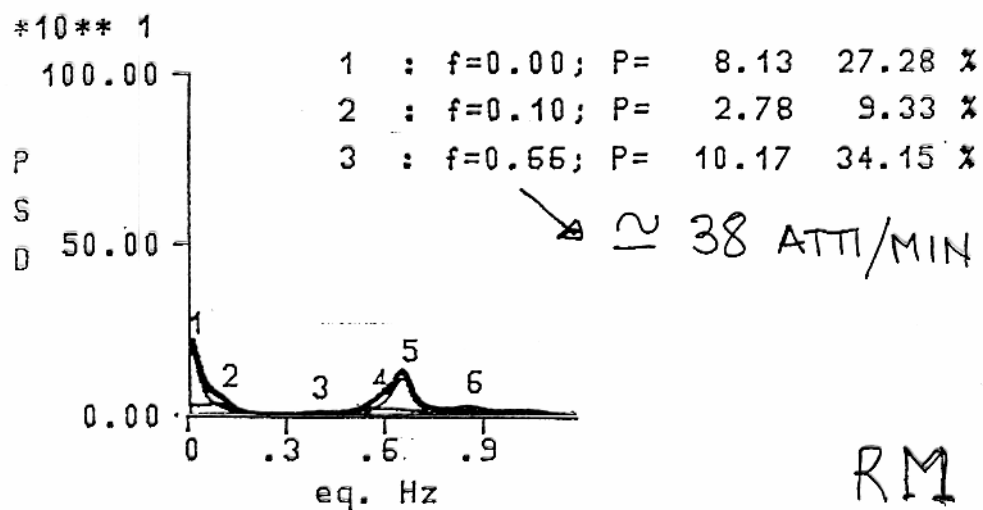
Compressed spectral array del segnale respiro registrato da un feto di pecora.

L'attività respiratoria iniziale è seguita da una fase di non respiro

Variabilità cardiaca fetale



Q



RM